

RESEARCH

Open Access



Divergent roles of ADP-ribosylation factor GTPase-activating proteins in lignocellulose utilization of *Trichoderma guizhouense* NJAU4742

Tuo Li^{1,2}, Qin Wang^{1,2}, Yang Liu^{1,2}, Jiaguo Wang^{1,2}, Han Zhu^{1,2}, Linhua Cao^{1,2}, Dongyang Liu^{1,2*} and Qirong Shen^{1,2}

Abstract

Background The ability of lignocellulose degradation for filamentous fungi is always attributed to their efficient CAZymes system with broader applications in bioenergy development. ADP-ribosylation factor GTPase-activating proteins (Arf-GAPs), pivotal in fungal morphogenesis, lack comprehensive studies on their regulatory mechanisms in lignocellulose utilization.

Results Here, the orthologs (*TgGlo3* and *TgGcs1*) of Arf-GAPs in *S. cerevisiae* were characterized in *Trichoderma guizhouense* NJAU4742. The results indicated that overexpression of *Tggcs1* (OE-*Tggcs1*) enhanced the lignocellulose utilization, whereas increased expression of *Tgglo3* (OE-*Tgglo3*) elicited antithetical responses. On the fourth day of fermentation with rice straw as the sole carbon source, the activities of endoglucanase, cellobiohydrolase, xylanase, and filter paper of the wild-type strain (WT) reached 8.20 U mL⁻¹, 4.42 U mL⁻¹, 14.10 U mL⁻¹, and 3.56 U mL⁻¹, respectively. Compared to WT, the four enzymes activities of OE-*Tggcs1* increased by 7.93%, 6.11%, 9.08%, and 12.92%, respectively, while those decreased to varying degrees of OE-*Tgglo3*. During the nutritional growth, OE-*Tgglo3* resulted in the hyphal morphology characterized by sparsity and constriction, while OE-*Tggcs1* led to a notable increase in vacuole volume. In addition, OE-*Tggcs1* exhibited higher transport efficiencies for glucose and cellobiose thereby sustaining robust cellular metabolic rates. Further investigations revealed that *Tgglo3* and *Tggcs1* differentially regulated the transcription level of a dynamin-like GTPase gene (*Tggtp*), eliciting distinct redox states and apoptotic reaction, thus orchestrating the cellular response to lignocellulose utilization.

Conclusions Overall, these findings underscored the significance of *TgArf-GAPs* as pivotal regulators in lignocellulose utilization and provided initial insights into their differential modulation of downstream targets.

Keywords Arf-GAPs, *Trichoderma*, Lignocellulose utilization, Cellular responses, Regulators

Background

Fungi of the genus *Trichoderma* are among the most prevalent soil fungi in nature, frequently inhabiting plant root ecosystems, and play a pivotal role in promoting plant growth and resisting soil-borne pathogens [1, 2]. Similar to other heterotrophs, *Trichoderma* spp. usually rely on particular host organisms or substrates for

*Correspondence:

Dongyang Liu
liudongyang@njau.edu.cn

¹ Key Lab of Organic-Based Fertilizers of China and Jiangsu Provincial Key Lab for Solid Organic Waste Utilization, Nanjing, China

² Nanjing Agricultural University, Nanjing 210095, Jiangsu, China



© The Author(s) 2024. **Open Access** This article is licensed under a Creative Commons Attribution-NonCommercial-NoDerivatives 4.0 International License, which permits any non-commercial use, sharing, distribution and reproduction in any medium or format, as long as you give appropriate credit to the original author(s) and the source, provide a link to the Creative Commons licence, and indicate if you modified the licensed material. You do not have permission under this licence to share adapted material derived from this article or parts of it. The images or other third party material in this article are included in the article's Creative Commons licence, unless indicated otherwise in a credit line to the material. If material is not included in the article's Creative Commons licence and your intended use is not permitted by statutory regulation or exceeds the permitted use, you will need to obtain permission directly from the copyright holder. To view a copy of this licence, visit <http://creativecommons.org/licenses/by-nc-nd/4.0/>.

their nutrition. During the colonization process in different habitats, including soils and roots, *Trichoderma* spp. can secrete copious amounts of lignocellulases to efficiently degrade plant residues, thereby acquiring sufficient energy resources [3]. Due to this characteristic, *Trichoderma* consistently demonstrates the capacity to assimilate nutrients and undergo prolific proliferation within intricate environmental settings. In recent years, researchers have extended the capacity of *Trichoderma* to secrete lignocellulases into the chemical engineering realm, focusing on producing innovative biofuels using cellulose waste materials [4]. In addition, new applications in several other fields have been identified for lignocellulases, including papermaking, textile production, composting, and animal feed [5]. In this context, a comprehensive investigation into the regulatory mechanisms of lignocellulose utilization in *Trichoderma* becomes particularly meaningful for understanding beneficial plant-microbe colonization and the various industrial and biotechnological applications of lignocellulases.

Natural lignocelluloses contain both crystalline and amorphous forms of celluloses, as well as hemicelluloses with complex structures and sugar components. This complexity makes the strategies used by filamentous fungi to degrade lignocellulose highly intricate [6]. Filamentous fungi involved in lignocellulose degradation can typically secrete over 20 different carbohydrate-active enzymes (CAZymes), including glycoside hydrolases (GHs), polysaccharide lyases (PLs), carbohydrate esterases (CEs), and auxiliary enzymes (AAs), to effectively synergize in the breakdown of these substrates [7]. Recent years, significant advancements have been made in the field of cellulase research, aimed at enhancing the efficiency of biomass hydrolysis. This includes the optimization of cellulase production, the development of culture medium formulations and fermentation processes, the engineering design of microbial characteristics for cellulase production, and protein engineering [8]. Moreover, effective substrate degradation also needs to consider other physical and chemical factors, including the lignin structure and content of the substrate, the accessibility of the substrate to cellulases, and the liquefaction capacity of enzymes or enzyme mixtures at different substrate concentrations [9, 10]. The regulation of CAZymes secretion in *Trichoderma* involves multiple pathways, and the current predominant research approaches mainly revolve around direct transcriptional regulation (transcription factors), upstream regulation through nutrient sensing pathways, and feedback regulation stemming from the secretion pathway [11]. While it has been established that lignocellulose degradation reactions are subject to strict transcriptional control, there is no doubt that

the ability of filamentous fungi to respond to environmental signals, such as dimorphism, will affect their substrate utilization capabilities. Many reports have indicated that fungal morphological changes triggered by signal transduction are crucial for their growth and development, influencing the secretion of extracellular hydrolytic enzymes [12, 13]. However, the impact of these signal transduction and response pathways on the utilization of lignocellulosic substrates in *Trichoderma* has never been assessed.

Usually, small GTPases act as signal transducers in eukaryotes to regulate various cellular functions including cytoskeletal regulation, cell proliferation and differentiation, and membrane trafficking [14]. At least five prominent families of small GTPases, including Ras, Rho/Rac, Rab, Arf, and Ran [15]. ADP-ribosylation factors (Arfs) represent a class of small GTPase proteins primarily engaged in orchestrating vesicle assembly and transport processes. They are composed of three subfamilies, containing Arf, Arf-like (Arl) and Sar proteins. Among these, more than 20 Arl and Arf proteins display a high degree of homology across various species [16]. Their initial characterization was closely linked to regulating cholera toxin activity [17]. Subsequent studies have indicated that Arfs are primarily associated with vesicle transport in the secretory pathway in *S. cerevisiae* [16]. Besides, Arf proteins are also involved in regulating mitochondrial morphology and function, as well as the biogenesis of organelles like peroxisomes [18, 19]. While the functions of Arf-GAPs in other fungi have been extensively elucidated, their role in *Trichoderma* requires further profound studies.

Trichoderma guizhouense NJAU4742, an efficient lignocellulose degrader and beneficial plant fungus, was extensively employed for the large-scale production of biofertilizers via co-solid-state fermentation with agricultural crop residues in China [20, 21]. In this study, the orthologs of Arf-GAP-Glo3p (*TgGlo3*) and Arf-GAP-Gcs1p (*TgGcs1*) in *S. cerevisiae* were characterized in NJAU4742, and their potential roles in influencing the lignocellulose utilization were preliminarily determined. Based on the genetic manipulation, enzymatic assays, and omics analyses, we provided further evidence that *TgGlo3* and *TgGcs1* could impact the efficiency of lignocellulose utilization by modulating glucose transport, hypha (vacuole) morphology, redox status, and the extent of cellular apoptosis. This study not only deepens our insights into the secretion mechanisms of lignocellulases in *Trichoderma*, but also provides a novel perspective on the potential of these fungi for applications in industry and biotechnology. On the other hand, these findings underscore the importance of Arf-GAPs as key regulatory factors in the utilization of lignocellulose. In future

research, we may be able to enhance the productivity of lignocellulases and promote the circular bioeconomy by rationally engineering the Arf-GAPs in filamentous fungi.

Results

TgGlo3 and *TgGcs1* differentially regulate lignocellulose utilization in NJAU4742

The orthologs of *Gcs1* and *Glo3* from *S. cerevisiae* were identified in the NJAU4742 genome through sequence retrieval and alignment. *TgGlo3* and *TgGcs1* each comprise 478 and 366 amino acid residues, and both possess conserved Arf-Gap domains (Fig. 1a). By constructing

phylogenetic trees, the results indicated that *TgGlo3* shared high homology with *Glo3* from other fungi, while *TgGcs1* exhibited a certain degree of species specificity (Fig. S1). To assess the impact of *TgGlo3* and *TgGcs1* on lignocellulase secretion, we initially attempted to generate deletion mutants in NJAU4742. After multiple attempts, it was impossible to generate a deletion mutant for *TgGlo3*, suggesting its essential role in the processes of primary life metabolism. Conversely, deletion mutants for *TgGcs1* ($\Delta Tggcs1$) were successfully obtained, which exhibited sparse mycelium growth, slow development, and pale-yellow spores (Fig. S2a). Due to the inability to

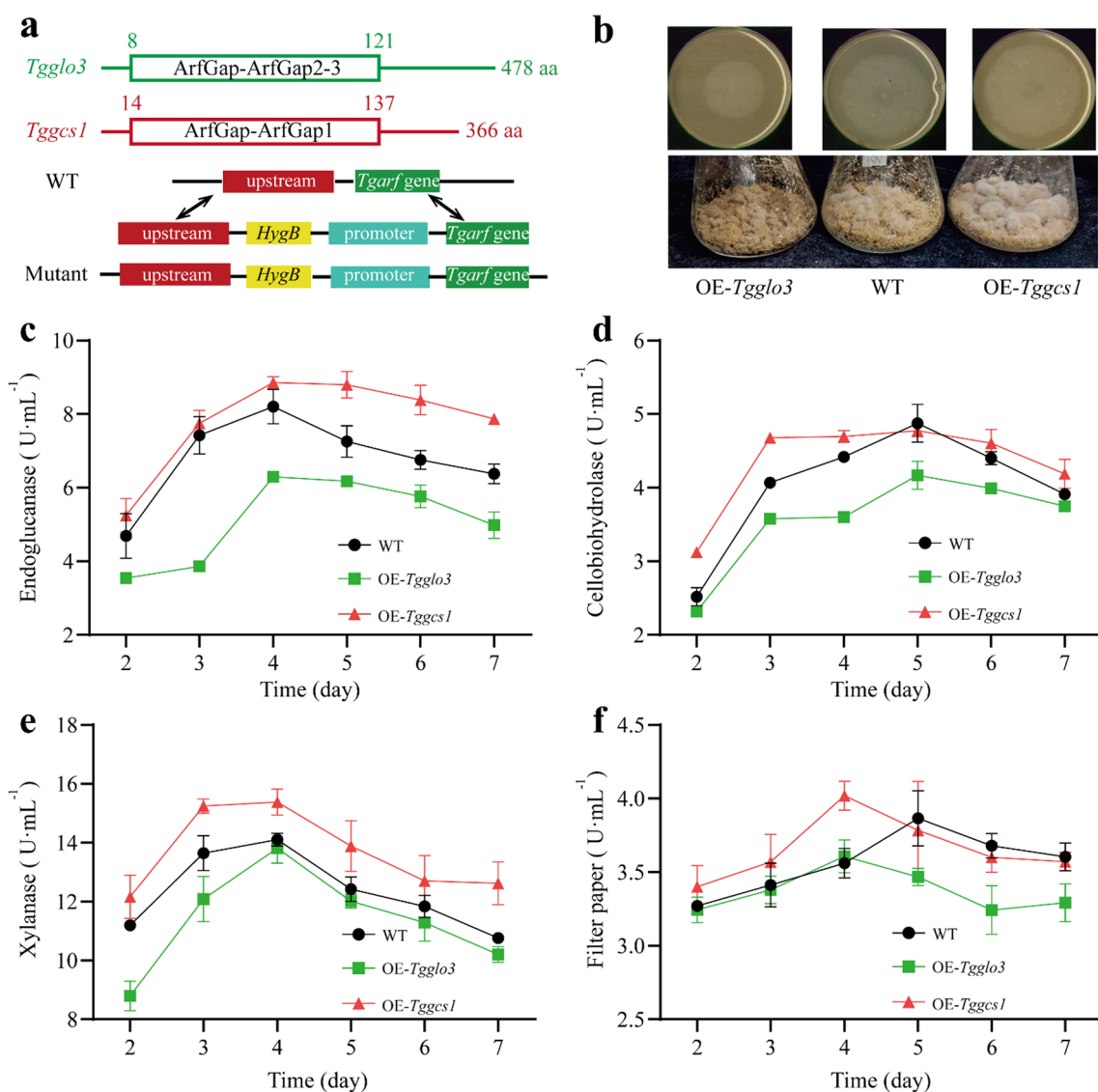


Fig. 1 Potential effect of *TgGlo3* and *TgGcs1* on the lignocellulolytic response of NJAU4742. **a** Domains and overexpression strategy of *TgGlo3* and *TgGcs1* in NJAU4742. **b** Growth of WT, OE-*Tggl03*, and OE-*Tggcs1* on plates and solid-state fermentation (SSF) when using straw as the sole carbon source. **c-f** Lignocellulase activities, including endoglucanase, cellobiohydrolase, xylanase, and filter paper activities, of WT, OE-*Tggl03*, and OE-*Tggcs1* during the fermentation process

simultaneously generate deletion mutants, we employed an overexpression approach by inserting a strong promoter (the promoter of Histone H4 in NJAU4742) to construct overexpression mutants (OE-*Tgglo3* and OE-*Tggcs1*). Both overexpression strains exhibited higher expression levels of their respective gene compared to WT (Fig. S2b), and their abilities to utilize lignocellulose were further evaluated.

Interestingly, OE-*Tgglo3* and OE-*Tggcs1* exhibited strikingly different lignocellulose utilization efficiencies compared to wide type (WT). Both in rice straw plates and solid-state fermentation (SSF), the growth of OE-*Tggcs1* surpassed that of WT, whereas the growth of the OE-*Tgglo3* was significantly inhibited (Fig. 1b). This was confirmed in liquid fermentation, where during the fermentation process using rice straw as the sole carbon source, the biomass of OE-*Tgglo3* was significantly inhibited, while the biomass of OE-*Tggcs1* was significantly increased from the third to the sixth day (Fig. S3). Meanwhile, different lignocellulase activities were measured to evaluate their impact on lignocellulases secretion. As shown in Fig. 1c, the endoglucanase activity in the WT, OE-*Tgglo3*, and OE-*Tggcs1* followed a similar trend. On the fourth day, the OE-*Tggcs1* reached its maximum activity (8.85 ± 0.17 U mL⁻¹), while OE-*Tgglo3* exhibited the lowest activity (6.29 ± 0.16 U mL⁻¹). The cellobiohydrolase activity fluctuated among different strains and peaked on the fifth day. Notably, there were little differences between WT and OE-*Tggcs1*, but the activities in OE-*Tgglo3* were significantly inhibited (Fig. 1d). By comparison, the xylanase activities rapidly increased in all treatments, with OE-*Tggcs1* consistently exhibiting the highest activities, maintaining a significant lead throughout the entire fermentation process (Fig. 1e). As for the filter paper activities, OE-*Tggcs1* rapidly increased and then slowly decreased, and peak was reached on the fourth day (4.02 ± 0.10 U mL⁻¹). In contrast, the activity of OE-*Tgglo3* slowly increased from days 1 to 4, after which it declined to a lower level (Fig. 1f). In summary, these results indicated that *TgGlo3* and *TgGcs1* exhibited contrasting roles in regulating the utilization of lignocellulose. Increased expression of *Tgglo3* was detrimental to the lignocellulose utilization for NJAU4742, while *Tggcs1* had the opposite effect.

***TgGlo3* and *TgGcs1* jointly influence spore germination and mycelial growth**

Fungi mainly rely on the perception and transmission of environmental signals for their growth and development, with Arf-GAPs playing crucial regulatory roles in this process [22]. To validate whether *TgGlo3* and *TgGcs1* exhibit different response patterns to lignocellulosic substrates, we examined spore germination and mycelial

developmental morphology separately in OE-*Tgglo3* and OE-*Tggcs1*, respectively. Surprisingly, during spore germination, the increased expression of both *Tgglo3* and *Tggcs1* was beneficial for the rapid germination and elongation of NJAU4742. At 16 h, the germination efficiency of the mycelium of OE-*Tgglo3* was particularly prominent compared to WT, with most spores germinated and beginning hyphal extension. At 20 h, the germination advantage of mycelium in OE-*Tgglo3* still existed, mainly manifested in the germination rate of spores and the density of mycelium. However, after 24 h, the advantage of hyphal elongation of OE-*Tggcs1* gradually emerged (Fig. 2a). This suggested that the expression of *Tgglo3* and *Tggcs1* might play a role in promoting the germination and growth of NJAU4742, potentially enhancing the efficiency of the germination process and the subsequent development of the mycelium. During the nutritional growth phase of the mycelium, the germination advantage of OE-*Tgglo3* disappeared, and the mycelia exhibited an unhealthy state, characterized by thin and shrunken morphology when using straw as the sole carbon source. On the contrary, the mycelia of OE-*Tggcs1* showed a similar overall morphology with WT, with the notable difference being that the volume of individual cells within the hyphae was larger (Fig. 2b). These results suggested that *TgGlo3* and *TgGcs1* exhibited different mycelial morphological regulatory patterns in NJAU4742 using lignocellulose as the sole carbon source, which might directly impact the production of lignocellulases.

***TgGcs1* dominates glucose absorption and vacuole morphology**

Morphological changes in mycelium are often closely related to energy metabolism, depending on the efficiency of the fungus in utilizing different soluble substrates [23]. Due to glucose being the preferred substrate for energy metabolism, the glucose fluorescent indicators were constructed to accurately measure the intracellular glucose concentrations among different strains. As shown in Fig. 2c, the glucose sensors exhibited two types of fluorescence, and the ratio of YFP/CFP indicated the concentration of glucose. Compared to WT (0.92), the ratio of YFP/CFP slightly decreased in OE-*Tgglo3* (0.87), while it showed a 2.5-fold increase in OE-*Tggcs1* (2.34) (Fig. 2d–f). Extensive microscopic sample analysis results confirmed the same trend, with the YFP to CFP ratio being close to 1.0 in WT and OE-*Tgglo3* while significantly increasing in OE-*Tggcs1*. These results indicated that the increased expression of *Tggcs1* promoted the accumulation of intracellular glucose, which was beneficial for mycelial growth and morphogenesis. However, when glucose was the sole carbon source, we observed

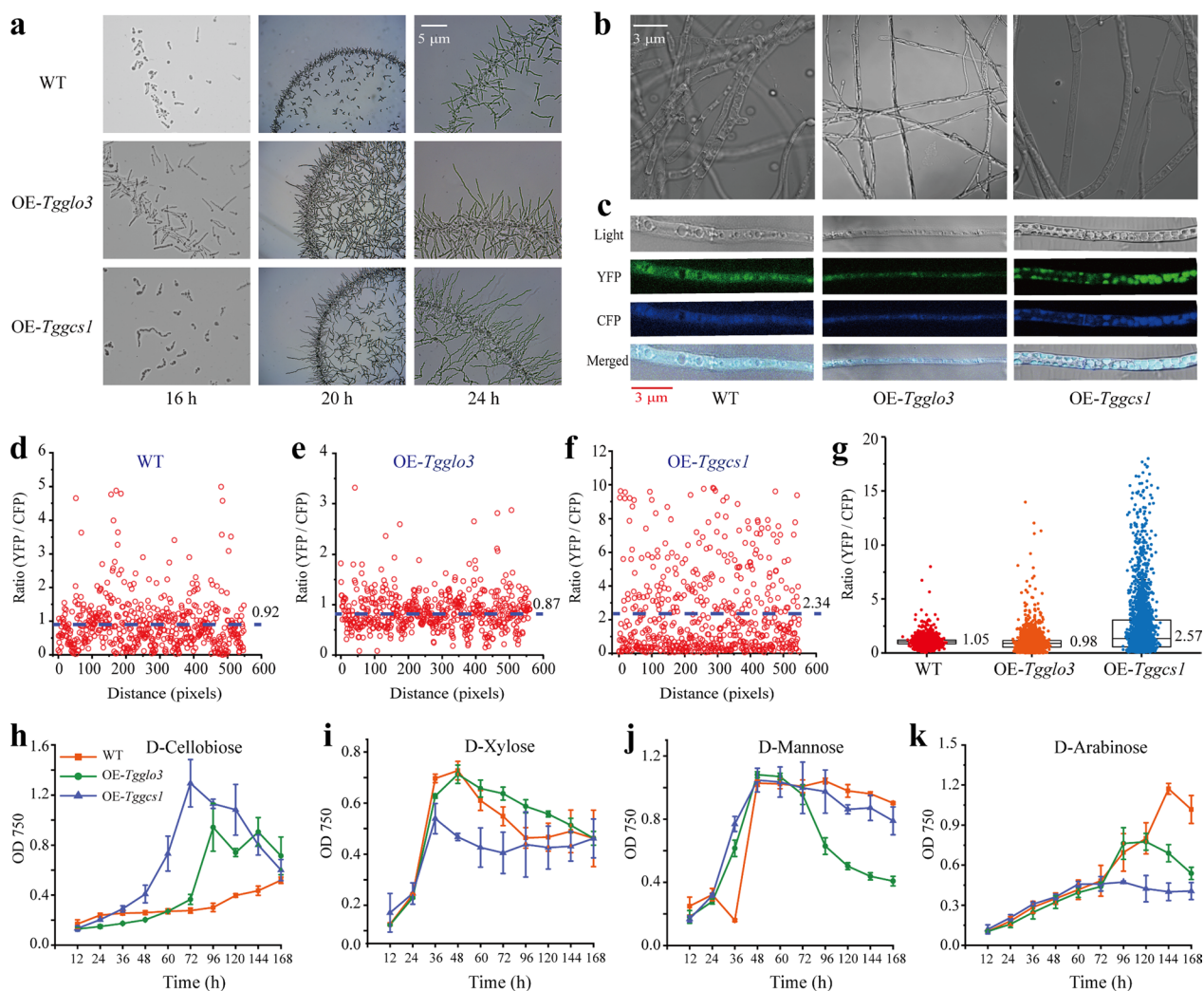


Fig. 2 Effects of *TgGlo3* and *TgGcs1* on spore germination, mycelial growth, and sugar transport efficiency. **a** Spore germination of WT, OE-*Tgglo3*, and OE-*Tggcs1* on PDA medium from 16 to 24 h, and bar = 5 μ m. **b** Mycelial growth of WT, OE-*Tgglo3*, and OE-*Tggcs1* on rice straw plates for 48 h, and bar = 3 μ m. **c** Confocal imaging monitoring of hyphae from WT, OE-*Tgglo3*, and OE-*Tggcs1* after being transferred the FRET glucose sensors (pDRf1-GW), and bar = 3 μ m. YFP was represented by green, and CFP was represented by blue, and the merged images were combined with YFP, CFP and Light. **d-f** Glucose levels plotted for single pixels of the mycelia expressing the glucose sensor in WT, OE-*Tgglo3*, and OE-*Tggcs1*. The YFP/CFP ratio of each pixel point was counted and the mean value was used as a measure of intracellular glucose levels. **g** Ratios of the YFP/CFP emission intensities of more mycelial samples in different strains, and the median was utilized to assess glucose levels. **h-k** Monitoring the utilization efficiency of different strains for various carbon sources by using Biolog FF Microplates, such as D-Cellobiose (**h**), D-Xylose (**i**), D-Mannose (**j**), and D-Arabinose (**k**). Three independent biological experiments were performed and the data was collected. Error bars represent \pm SDs

that OE-*Tggcs1* did not exhibit a higher biomass (Fig. S4), which might seem illogical. Nevertheless, it was important to note that when lignocellulose was used as a substrate, OE-*Tggcs1* secreted more lignocellulases, producing more glucose. In contrast, OE-*Tgglo3* was limited in the production of lignocellulases, resulting in less extracellular glucose, thus creating a difference in the accumulation of intracellular glucose. Given the complexity of lignocellulosic substrates,

further investigations into the relationship between additional degradation products and strain growth were explored. Among these, OE-*Tggcs1* significantly improved the ability to utilize D-cellobiose, OE-*Tgglo3* exhibited a slight advantage in D-xylose utilization, while D-Mannose and D-Arabinose increased the biomass of WT in the late stage of cultivation (Fig. 2h–k). The above results indicated that changes in the expression levels of *Tgglo3* and *Tggcs1* might interfere with

the absorption efficiency of NJAU4742 in different substrates, and increased expression of *Tggcs1* mediated the transport of glucose and cellobiose.

The morphology of vacuoles is closely related to hyphal polar growth but also affects the secretion of extracellular lignocellulases [24, 25]. Besides, the extensive vacuole expansion can substitute for cytoplasmic biosynthesis under nutrient scarcity, occurring with minimal biosynthetic demands, leading to tip expansion and cellular movement [26]. The observation results of TEM indicated that *Tggcs1*, rather than *Tgglo3*, played a significant role in mediating the changes in vacuole morphology in NJAU4742, especially in terms of size (Fig. 3a). Given that vacuole volume occupied a significant portion of the total volume in the fungal cell, this might explain the increased volume of individual cells observed in OE-*Tggcs1*. On the other hand, previous reports suggested that under fungal secretion conditions, there was an increase in both the average size and concentration of vacuoles [24]. Therefore, combining previous research with the current findings, we could reasonably infer that the increased expression of *Tggcs1* enhanced the efficiency of lignocellulase secretion by altering cell vacuole morphology.

TgArfs mediate oxidative stress and apoptosis

Our previous research indicated that ATP synthesis occurred simultaneously with oxidative stress within NJAU4742, and this relationship was closely associated with intracellular glucose concentrations [27]. Considering the differences in intracellular glucose accumulation, we conducted preliminary assessments of the oxidative–reductive states in different strains using straw as the sole carbon source. The results indicated a significant decrease in the content of GSSG in OE-*Tgglo3*, while there was little change in OE-*Tggcs1* compared to WT. On the contrary, the contents of GSH were significantly increased in OE-*Tgglo3* and OE-*Tggcs1*, resulting in lower GSSG/GSH ratios (Fig. 3b). High GSSG/GSH ratio in metabolic processes can lead to oxidative stress, which is often associated with ROS production [28]. The fluorescence probe DCFH-DA for visualizing and quantifying ROS in different strains indicated that ROS levels were significantly reduced in OE-*Tgglo3* and OE-*Tggcs1* (Fig. 3c, d). This might appear paradoxical, given the significant accumulation of glucose in the OE-*Tggcs1* compared to WT. Elevated glucose levels would typically stimulate increased metabolic activity, which would induce ROS production in turn. Therefore, there might be a novel mechanism involving *TgArfs* in regulating

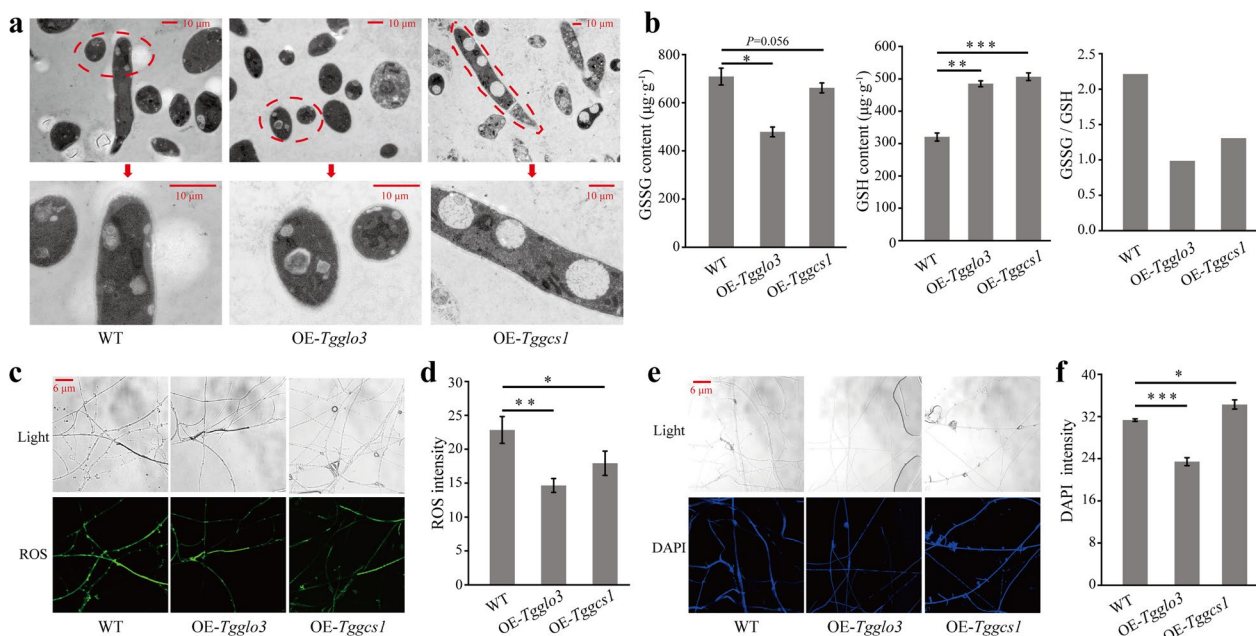


Fig. 3 Multiple effects triggered by *Tgglo3* and *Tggcs1* in response to lignocellulose. **a** Transmission electron micrographs showing vacuoles in WT, OE-*Tgglo3*, and OE-*Tggcs1*. Shown are representatives of at least 5 images. **b** Intracellular levels and ratios of oxidized glutathione (GSSG) and reduced glutathione (GSH). **c** Confocal imaging of hyphae from WT, OE-*Tgglo3*, and OE-*Tggcs1* after staining with DCFH-DA fluorescence probe, and bar = 6 μm. **d** Evaluation of the ROS content by analyzing the fluorescence intensity of WT, OE-*Tgglo3*, and OE-*Tggcs1*. **e** Confocal imaging of hyphae from WT, OE-*Tgglo3*, and OE-*Tggcs1* after staining with DAPI, and bar = 6 μm. **f** Relative apoptosis levels of were evaluated via DNA condensation on DAPI staining in different strains. Data were calculated from at least three biological replicates, and error bars represent ± SDs. * $P < 0.05$, ** $P < 0.01$, *** $P < 0.001$. A P value < 0.05 was regarded as statistically significant

intracellular redox levels in fungal cells, particularly during the process of lignocellulose utilization.

Prior reports indicated that the decrease in glucose transport resulted from declining cell viability and a significant component of the apoptosis process [29]. Hence, we speculated that the variations in intracellular glucose levels, primarily governed by *Tgglo3* and *Tggcs1*, were closely related to cell apoptosis. Firstly, the relative apoptosis levels were evaluated via DNA condensation on DAPI staining. As expected, there were significant differences among the three strains, and OE-*Tgglo3* showed a decrease of approximately 25%, while OE-*Tggcs1* increased by about 10% compared to WT (Fig. 3e, f). Simultaneously, the activity of caspase-3, which served as an indicator of the level of cellular apoptosis, was assessed. In line with the DAPI staining results, the activity of caspase-3 displayed distinct trends in *Tgglo3* and *Tggcs1*. When normalized the caspase-3 activity to 1.00 in WT, the activity in OE-*Tgglo3* decreased to 0.77 while increased to 1.32 in OE-*Tggcs1* (Fig. S5a). It is important to note that the balance between cell proliferation and apoptosis is crucial for growth and development. In other words, rapid cell proliferation is often accompanied by faster cell apoptosis [30]. Furthermore, increased cellular metabolism enhances substrate utilization, leading to carbon source scarcity and potentially accelerating cellular apoptosis. Therefore, combining the previous results, we could reasonably speculate that the high expression of *Tggcs1* facilitated the rapid utilization of carbon sources and efficient glucose absorption by the cells, thus promoting rapid cell proliferation and apoptosis, while the high expression of *Tgglo3* played a negative role.

Transcriptomic analysis of different strains under SSF

To further investigate the underlying mechanisms through which *Tgglo3* and *Tggcs1* influence the lignocellulose utilization by NJAU4742, the 4-day-old mycelia of different strains under SSF were used as transcriptomic samples. The gene expression levels were evaluated by performing quality control and sequencing analysis, and a criteria of $|\log_2\text{Fold Change}| \geq 1$ and q value < 0.05 was used to assess the changes between different samples. As shown in Fig. 4a, 1885 and 2619 genes were significantly upregulated and downregulated in OE-*Tgglo3* compared to WT. In comparison, the overexpression of *Tggcs1* led to more pronounced changes in gene expression levels, with 3663 and 2516 genes showing substantial increases and decreases in expression in OE-*Tggcs1* relative to WT, respectively (Fig. 4b). Gene Ontology (GO) annotation results indicated that the differentially expressed genes regulated by *Tgglo3* and *Tggcs1* were mainly associated with catalytic activity and oxidation–reduction processes (Fig. 4c). This appeared to explain why OE-*Tgglo3*

and OE-*Tggcs1* exhibited different substrate degradation enzyme activities and distinct oxidation–reduction states. The differential heat map of gene clustering provided a visual representation of gene expression under different treatments. Compared to WT, there were 21 genes (R1) that significantly upregulated only in OE-*Tggcs1*, and 41 genes (R2) showed a higher level of upregulation in OE-*Tggcs1*. Furthermore, 22 genes (R3) were downregulated with the increasing expression levels of *Tgarfs*, and 12 genes (R5) were significantly upregulated in OE-*Tgglo3*, with no significant changes in OE-*Tggcs1*. It was worth noting that there were 4 genes (R4) whose expression levels exhibited completely opposite trends in OE-*Tgglo3* and OE-*Tggcs1*, including A1A102823 (*Tgexp*), A1A106746 (*Tghyp1*), A1A104094 (*Tghyp2*), and A1A100231 (*Tggtp*). They were significantly upregulated in OE-*Tgglo3* while being significantly suppressed with the increasing expression levels of *Tggcs1* (Fig. 4d). Considering the completely opposite performance of OE-*Tgglo3* and OE-*Tggcs1* in utilizing lignocellulose, we reasonably speculated that the upregulation of *Tgglo3* and *Tggcs1* might exert downstream regulation by influencing the expression levels of R4.

Tggtp is differentially regulated by *Tgglo3* and *Tggcs1*

Sequence alignment and functional retrieval determined that *Tghyp1* and *Tghyp2* encode hypothetical proteins. In addition, *Tgexp* and *Tggtp* encode expansin and dynamine-like GTPase, respectively. The acquisition of valuable information regarding protein functionality encoded by genes is insufficient. Subsequently, different gene deletion mutants were generated, and their respective abilities to utilize lignocellulose were initially assessed. As depicted in Fig. 5a, $\Delta Tggtp$ exhibited the most conspicuous growth advantage during SSF compared to WT. Simultaneously, the lignocellulases activities were assayed during the co-fermentation of different strains with rice straw. The results elucidated that endoglucanase activity exhibited varying degrees of enhancement in different mutants, while the activity of cellobiohydrolase remained relatively stable compared to WT. For xylanase and filter paper activity, $\Delta Tggtp$ prominently demonstrated advantageous performance within the initial 4 days of fermentation (Fig. 5b). Meanwhile, overexpression mutant of *Tggtp* (OE-*Tggtp*) was constructed, and the corresponding lignocellulases activities were determined. As expected, various enzymatic activities of OE-*Tggtp* were significantly inhibited to different degrees compared to WT (Fig. 5c). Consequently, the attenuation of *Tggtp* expression exerted a regulatory influence on improving lignocellulose utilization by amplifying the lignocellulases activities of NJAU4742. Furthermore, it was noteworthy that transcription levels of *Tggtp* were positively and

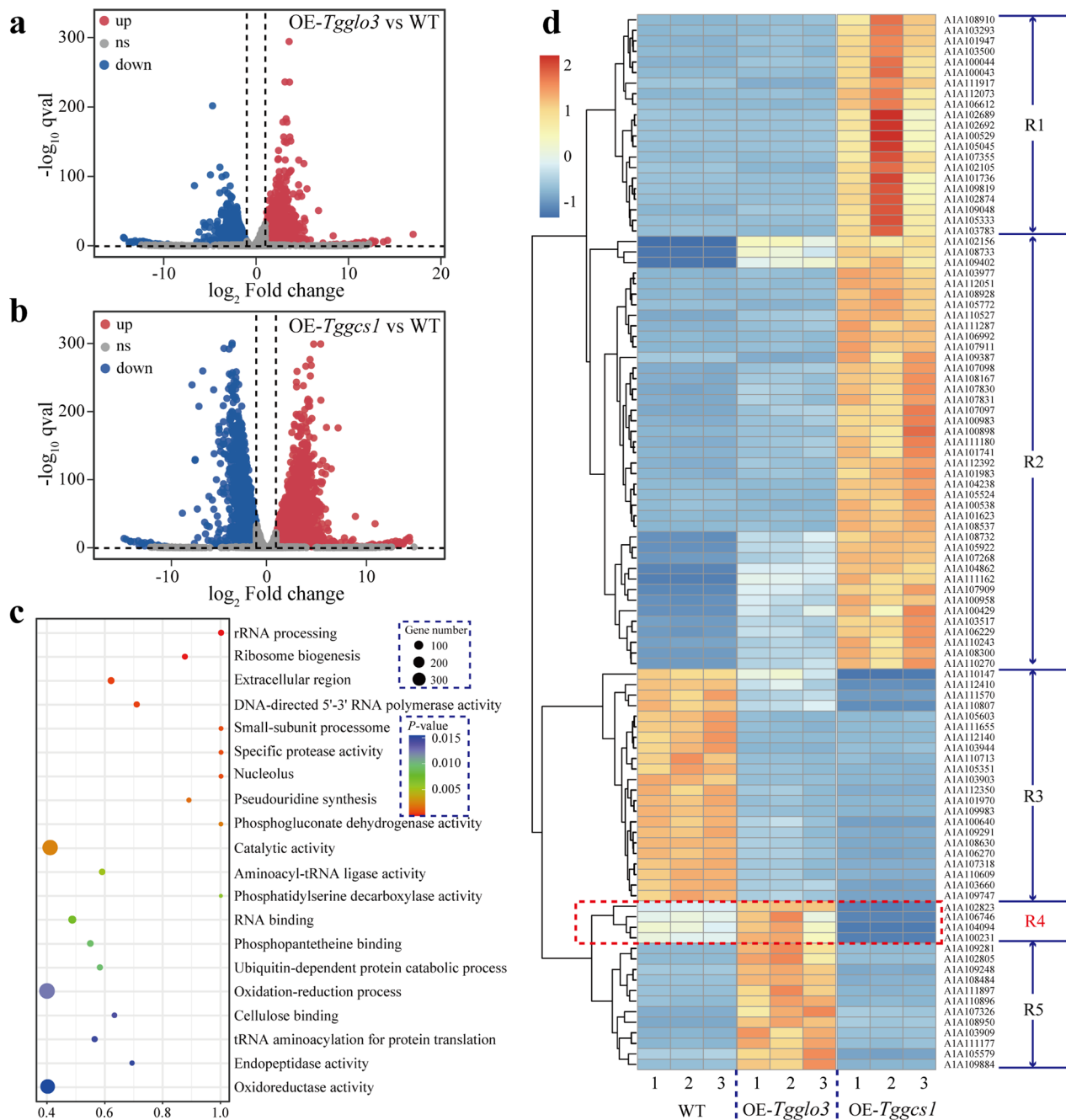


Fig. 4 Transcriptome analysis of different strains including WT, OE-*Tgglo3*, and OE-*Tggcs1* in response to lignocellulose. **a, b** Distribution of significantly up/down-regulated genes ($|\log_2\text{Fold Change}|\geq 1$ and q value < 0.05) of OE-*Tgglo3*, and OE-*Tggcs1* relative to WT. The q value was plotted against the expression fold change of all detected genes within the different groups. Data points in the lower center area of the plots (grey circles) display unchanged or proteins with no significant fold change. Data points in the upper quadrants indicate genes with significant negative (blue circles) and positive (red circles) changes in gene abundances. **c** GO annotation of differentially expressed genes in different strains. The size of the circle correlates with the number of genes and the color represents the P value. **d** Hierarchical cluster analysis of the differentially expressed genes in different treatments. The heat map was divided into five regions (R1–R5) according to the differences in gene expression

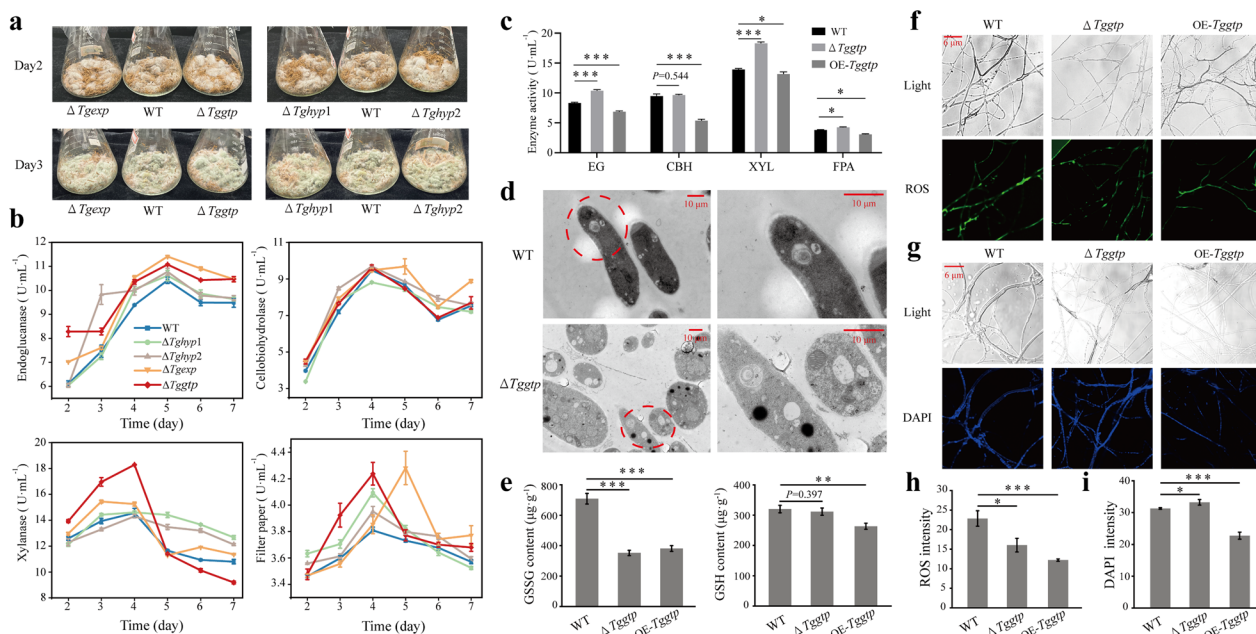


Fig. 5 *Tgglo3* and *Tggc1* trigger distinct cellular responses in coping with lignocellulose utilization by differentially regulating the transcriptional level of *Tggtp*. **a** Growth of different gene deletion strains during SSF. **b** Lignocellulase activities, including endoglucanase, cellobiohydrolase, xylanase, and filter paper activities, of WT, $\Delta Tghyp1$, $\Delta Tghyp2$, $\Delta Tgexp$, and $\Delta Tggtp$ during the fermentation process. **c** Hydrolase activities, including EG, CBH, XYL, and FPA of WT, $\Delta Tgexp$, and OE-*Tggtp* by using rice straw as the sole carbon source. EG endoglucanase, CBH cellobiohydrolase, XYL xylanase, FPA filter paper activity. **d** Comparison of the vacuole morphology of mycelium from WT and $\Delta Tggtp$. **e** Intracellular levels of oxidized glutathione (GSSG) and reduced glutathione (GSH) in WT, $\Delta Tggtp$, and OE-*Tggtp*. **f, g** Confocal imaging of hyphae from WT, $\Delta Tggtp$, and OE-*Tggtp* after staining with DCFH-DA and DAPI, and bar = 6 μ m. **h, i** ROS and apoptosis assay based on the fluorescence intensity analysis. Data were calculated from at least three biological replicates, and error bars represent \pm SDs. * $P < 0.05$, ** $P < 0.01$, *** $P < 0.001$. A P value < 0.05 was regarded as statistically significant

negatively modulated by *Tgglo3* and *Tggc1*, respectively, which might elucidate the underlying rationale for the diametrically opposed outcomes observed in lignocellulose utilization between OE-*Tgglo3* and OE-*Tggc1*.

Vacuole morphology was initially characterized to further elucidate the linkage between *Tggtp* and *Tggc1*. Evidently, similar to the overexpression of *Tggc1*, the deletion of *Tggtp* also resulted in an increase in vacuole volume (Fig. 5d). In addition, at the hyphae apex of $\Delta Tggtp$, an increased presence of vesicle-like structures was observed. The formation of these vesicles was closely associated with the secretion of extracellular cellulases, as lignocellulose enzymes were typically transported to the extracellular environment encapsulated within vesicles [31]. Given the significant alterations in the cellular redox state resulting from the elevated expression levels of *Tgglo3* and *Tggc1*, thereby affecting the cell viability. Consequently, GSSG, GSH, and ROS levels were reevaluated in the mutant strains associated with *Tggtp*. It was evident that in OE-*Tggtp*, both GSSG and GSH levels were significantly lower than that in WT, whereas $\Delta Tggtp$ only exhibited a significant reduction in GSSG content (Fig. 5e). Overall, the ratio of GSSG to GSH was

decreased in $\Delta Tggtp$ and OE-*Tggtp* (Fig. S5b). This was an interesting observation, because the overexpression of *Tgglo3* and *Tggc1* did indeed lead to a reduction in the GSSG to GSH ratio, while *Tgglo3* and *Tggc1* showed opposite regulatory trends on the transcription levels of *Tggtp*. To ascertain whether the redox state was associated with ROS, the ROS levels in different strains were reevaluated through DCFH-DA staining. Consistent with the results of glutathione detection, the fluorescence intensity of ROS was significantly reduced in $\Delta Tggtp$ and OE-*Tggtp* (Fig. 5f, h). Finally, to investigate the potential association between *Tgarfs*-mediated apoptosis and *Tggtp*, the apoptotic levels in different strains were reevaluated through DAPI staining. The results revealed that, in accordance with the findings in the *Tgarfs* overexpression strains, $\Delta Tggtp$ displayed elevated levels of apoptosis, whereas OE-*Tggtp* exhibited a marked reduction (Fig. 5g, i). This suggested that, in the context of lignocellulose as the carbon source, cellular apoptotic status displayed a positive correlation with strain biomass, thus indirectly substantiating the notion that heightened levels of cellular apoptosis often coincided with more robust metabolic activities.

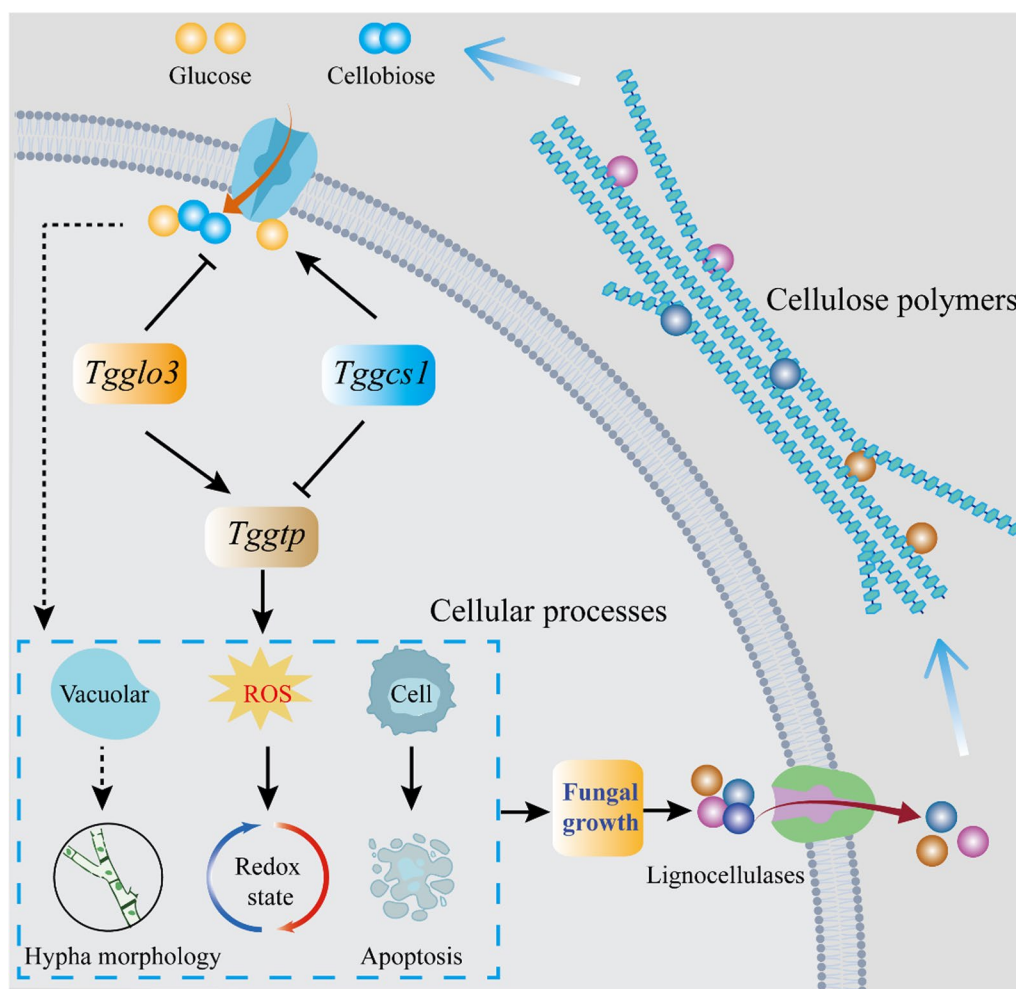


Fig. 6 Proposed model for *Tgglo3* and *Tggcs1* as pivotal regulators in lignocellulose utilization. During lignocellulose utilization, the expression of *Tgglo3* and *Tggcs1* was closely related to the intracellular content of glucose and cellobiose. Besides, *Tgglo3* and *Tggcs1* affected various cellular processes in response to lignocellulases secretion by differentially regulating the transcriptional level of *Tggtp* in NJAU4742

In summary, the results above indicated that the expression level of *Tggtp* was differentially regulated by *Tgglo3* and *Tggcs1*. Decreased expression of *Tggtp* contributed to the lignocellulases secretion, mediated through the modulation of vacuole morphology, redox state, and cell apoptosis status (Fig. 6).

Discussion

Saprophytic filamentous fungi typically acquire energy for reproduction and colonization by secreting lignocellulases to degrade plant residues [32]. It has been reported that plant growth-promoting rhizobacteria (PGPR) enhance their colonization on plant roots by secreting cellulases, leading to the expansion, lysis, and demise of pathogenic fungal cells [3]. Simultaneously, these degradative enzymes bolster their capacity to establish themselves on the plant root surface, thereby

promoting plant growth [33]. In recent years, lignocellulosic biomass has emerged as a rich and renewable resource, and the production of high-value compounds through the enzymatic degradation and utilization of lignocellulose has become a focal point in research and biotechnological applications [34]. Hence, the investigation of lignocellulase secretion by filamentous fungi has been a prominent area of focus. Numerous researchers have been dedicated to elucidating the regulatory mechanisms governing lignocellulase secretion in filamentous fungi, as well as striving to enhance and optimize the enzyme production efficiency, which will provide valuable targets for the engineering of lignocellulose-degrading fungi.

The transcription activation of lignocellulase genes is rigorously regulated by transcription factors. In *Trichoderma reesei* and *Aspergillus niger*, the primary transcriptional regulatory factor for cellulase and hemicellulase

is XYR1/XlnR [35, 36]. In *Neurospora crassa*, the transcription factor CLR-2 drives the expression of cellulase genes, and its homologous protein ClrB regulates cellulase gene expression in *Aspergillus nidulans* [37]. In addition, several environmental signals also exert regulatory control over lignocellulase secretion, with carbon catabolite repression (CCR) being a notable representative mechanism. In the presence of high-quality carbon sources available for direct microbial utilization, microbes typically repress the expression of specific non-essential functional genes. In filamentous fungi, CCR is governed by the zinc binuclear cluster transcription factor CreA/CRE1/CRE-1 [38]. Initially, CCR was thought to be associated with the inhibition linked to intracellular glucose levels, but in organisms capable of utilizing a variety of complex carbon sources, CCR has evolved to respond to a range of carbon sources [39]. Post-translational regulation of lignocellulase is another commonly studied mechanism. Previous reports have pointed out that when filamentous fungi are exposed to chemical stresses targeting the secretion system, the upregulation of HacA/HAC1/HAC-1 expression inhibits the transcription of lignocellulase genes [40]. While extensive research has been conducted on the transcriptional regulation of lignocellulase genes in filamentous fungi, it has remained unclear how key regulatory factors governing mycelial growth and development impact their utilization of lignocellulose when it is used as a carbon source. In this study, we characterized the ADP-ribosylation factors *Tgglo3* and *Tggcs1* in *Trichoderma guizhouense* NJAU4742 and elucidated their impact on lignocellulose utilization through multiple facets, including mycelial development, vacuole morphology, glucose transport, and redox status.

During the mycelial growth of filamentous fungi, the significance of small GTPases such as Ras and Rab had been extensively elucidated [41], whereas relatively less attention had been given to Arf-GAP. In this study, *Tgglo3* could not be successfully knocked out, and overexpression led to mycelial growth defects, indicating that the expression level of *Tgglo3* needed to be precisely controlled. In *Arthrotrichum oligospora*, the deletion of the *Aoglo3* resulted in growth defects and an increase in mycelial spacing [42]. Interestingly, the overexpression of *Tggcs1* led to a significant reduction in mycelial spacing (Fig. 2b). Hence, there may be functional overlap between *Tggcs1* and *Aoglo3*, possibly due to evolutionary differences between species. In addition, qPCR results revealed that the overexpression of *Tgglo3* and *Tggcs1* led to a significant decrease in the expression of another gene (Fig. S6), indicating potential functional redundancy between these two genes. However, the absence of *Tggcs1* did not disrupt the stable expression of *Tgglo3*, reaffirming

the significance of the stable expression of *Tgglo3*. On the other hand, filamentous fungi grow as highly polarized tubular cells, and the growth rate at the hyphal tip and cell wall expansion are closely linked to vesicle supply [43, 44]. During the early stages of hyphal growth, the overexpression of *Tgglo3* and *Tggcs1* both promote hyphal elongation, although it remains unclear whether this is associated with changes in vesicle morphology. In the later stages of development, the overexpression of *Tggcs1* significantly increased vacuole volume. When vacuoles were compressed in narrow hyphae, it raised the question of whether this would increase the volume of individual cells in the hyphae of OE-*Tggcs1*. On the other hand, previous report indicated that the secretion of cellulases by *Trichoderma reesei* might be associated with vacuoles [45]. One hypothesis was that these hydrolytic enzymes were stored in vacuoles in an inactive form to prevent the harmful effects of overproduction of cellulases within *Trichoderma reesei* cells [46]. Therefore, it was reasonable to speculate that when the vacuolar morphology of OE-*Tggcs1* became larger, this was to store more inactive cellulases to avoid excessive stress on the cells.

A recent study has indicated that efficient glucose transport in filamentous fungi can significantly enhance fermentation efficiency. Upregulation of glucose transport capacity also contributes to the efficient production of cellulases in microbial cell factories [47]. Consistently, elevated glucose levels within the mycelium of OE-*Tggcs1* were accompanied by more efficient lignocellulase production. Besides, overexpression of *Tgglo3* suppressed the transcription levels of two essential glucose transport proteins (OPB36822.1 and OPB45586.1), while the opposite was observed in OE-*Tggcs1* during the SSF process (Fig. S7). This suggested that *Tgarfs* might control glucose transport efficiency by influencing the expression levels of glucose transport proteins. Higher glucose transport capacity undoubtedly contributed to sustaining robust cell metabolism, particularly in CAZymes metabolism. In general, high intracellular glucose concentrations can trigger CCR, thereby upregulating Cre expression, and inhibiting cellulase gene expression in filamentous fungi [48]. However, this phenomenon did not occur in OE-*Tggcs1*, and a significant upregulation was observed in the expression of most key lignocellulase genes in OE-*Tggcs1* (Table S1), indicating that intracellular glucose concentrations in OE-*Tggcs1* were not sufficient to trigger CCR when using lignocellulose as the sole carbon source. In fact, the intracellular transport efficiency of lignocellulosic hydrolysis products (mainly glucose, xylose, and cellobiose) is a primary driver of enzyme production sustainability and secondary metabolism [47]. When lignocellulose is broken down into glucose, which accumulates

extracellularly, the cell will prioritize utilizing this glucose before continuing to produce lignocellulases, thus avoiding excessive energy expenditure. The increased glucose content within cells in OE-*Tggcs1* was likely due to the increased secretion of lignocellulases, generating more glucose. Consequently, OE-*Tggcs1* showed a higher accumulation of intracellular glucose, which to some extent was converted into biomass. However, it should be noted that under conditions of glucose sufficiency (i.e., where glucose is the only carbon source), this biomass advantage might no longer exist, as there was no need for the secretion of lignocellulases. On the other hand, previous research has shown that high glucose levels often occur concurrently with oxidative stress in *Trichoderma* under stress conditions [27]. This study revealed that the overexpression of *Tgglo3* and *Tggcs1* effectively reduced the levels of ROS and the GSSG/GSH ratio in NJAU4742, which was apparently contradictory. A reasonable inference was that the low ROS triggered by *Tgglo3* and *Tggcs1* was unrelated to intracellular glucose concentrations. However, the alterations in cellular metabolism induced by glucose transport are fully reflected in cell apoptosis. Under nutrient stress, fungal cells need constant turnover to maintain vitality [49]. Therefore, changes in intracellular glucose concentrations mediated by *Tggcs1* and *Tgglo3* might be coupled to cell apoptosis, affecting lignocellulose utilization.

Arf proteins have little intrinsic GTP hydrolysis activity, and while each protein has a specific GTPase-activating protein (GAP) companion, it merely elicits a reaction opposite to that of GEF [50]. In this study, we reported that *Tgglo3* and *Tggcs1* regulated a series of cellular responses by affecting the expression level of *Tggtt*, leading to differential responses in the utilization of lignocellulose. The dynamin-like GTPase, encoded by *Tggtt* in NJAU4742, is a member of the large GTPase dynamin superfamily. It possesses a GTP-binding domain at the N-terminus and a GTP effector domain at the C-terminus [51]. In *Phytophthora sojae*, the dynamin-related protein *PsVPS1* was involved in forming vacuolar morphology and cysts, and it played a crucial role in virulence and extracellular protein secretion [52]. In *Fusarium graminearum*, the dynamin-like GTPase protein *FgSey1* was essential for hyphal vegetative growth, DON production, and pathogenicity [53]. In addition, dynamin-like GTPases play a pivotal role in intracellular transport, particularly in the trafficking of materials associated with the endoplasmic reticulum (ER). For instance, the *Sey1*/atlastin family of dynamin-like GTPases is known to participate in the homotypic fusion of ER membranes [54]. On the contrary, our data suggested that NJAU4742 did not appear to rely on *Tggtt*, and the loss of *Tggtt* actually increased the lignocellulases secretion when using

cellulose as the sole carbon source. Consistently, it had been found that the deletion of *vps10*, *vps13*, and *vps21* enhanced cellulase production by reducing vacuolar transport and degradation, as well as by differentially regulating the expression of sugar transport protein in *Trichoderma reesei* [55]. Another study suggested that modifying the vacuolar protein sorting pathway by knocking out *vps* genes could enhance the secretion of extracellular proteins [56]. In addition, the blocking of early endosome sorting by deleting *vps8* and *vps21* increased carboxylesterase production by 80% in protease-deficient *Pichia pastoris* [57]. Therefore, *Tggtt* not only altered vacuolar morphology, but might potentially enhance its secretion by modifying the vacuolar transport process for lignocellulases in NJAU4742, while further in-depth research is still required to confirm these findings.

Conclusion

Arf-GAPs, as crucial regulatory factors influencing fungal cellular metabolism, remain relatively unexplored in *Trichoderma*, particularly in the context of lignocellulose utilization. Here, this study demonstrated that *Tgglo3* and *Tggcs1* could differentially regulate the expression of *Tggtt*, thereby affecting various biological processes such as glucose transport, hypha (vacuolar) morphology, redox status, and apoptosis levels in response to lignocellulose utilization. These findings will contribute to a better understanding of the mechanisms underlying lignocellulose utilization in filamentous fungi and hold the potential to advance the effective utilization of agricultural solid waste.

Materials and methods

Strains and culture conditions

Trichoderma guizhouense NJAU4742 was maintained at -80°C in 30% glycerol in our laboratory, and its genome sequence was already published in the NCBI database (accession No. LVVK00000000.1). Mandels' salt solution without organic components ($1.4\text{ g L}^{-1} (\text{NH}_4)_2\text{SO}_4$, $2.0\text{ g L}^{-1} \text{KH}_2\text{PO}_4$, $0.3\text{ g L}^{-1} \text{CaCl}_2$, $0.3\text{ g L}^{-1} \text{MgSO}_4$, $5\text{ mg L}^{-1} \text{FeSO}_4 \cdot 7\text{H}_2\text{O}$, $20\text{ mg L}^{-1} \text{CoCl}_2$, $1.6\text{ mg L}^{-1} \text{MnSO}_4$ and $1.4\text{ mg L}^{-1} \text{ZnSO}_4$) supplemented with 1.5% (w/v) rice straw was used for lignocellulase production under liquid fermentation [58]. The rice straw used in this study was obtained from the local farmland (Nanjing, China) and ground into powder using a pulverizer. Before fermentation, the straw was pretreated with NaOH to remove surface lignin. Briefly, straw samples were soaked in a 2.5% NaOH solution at a ratio of 1:10 (w/v) at room temperature for 2 h. After full reaction, the treated straw was thoroughly washed with deionized water and air-dried naturally. Finally, all treated straw was ground into

a powder using a mill and used as fermentation substrate. Spores were collected from the incubated PDA plates followed by the filtration through four gauze layers. The spore suspension was adjusted to 1.0×10^7 spores·mL⁻¹ by quantifying spores on a hemocytometer. All SSF treatments were performed at 28 °C for 7 days, with the moisture content adjusted to 75% (w/w) using Mandels' salt solution, and samples were collected at 2–7 days. Three biological repeats existed for each sampling point, and equally harvested biomass of different strains was transferred to rice straw medium to observe the growth rate and biomass.

Assays of biomass and enzyme activities

For biomass assay, the liquid fermentation mixtures were collected daily, and the total DNA was extracted with the EZNATM Soil DNA kit (Omega Bio-Tek, Inc., Norcross, GA, USA). The number of NJAU4742 copies was determined with SYBR Premix Ex Taq II (RR820A, Takara, Dalian, China), and the amplification of the fragment using the extracted DNA as a model was performed on a CFX Connect Real-Time System (Bio-Rad, Hercules, USA). For enzyme activities assay, filter paper activity and endoglucanase activity were measured with filter paper (Whatman NO.1) and CMC-Na (Sigma, USA) as the substrates [59, 60]. Xylanase activity was assayed with oat spelt xylan (Sigma, USA) as the substrates [61]. These three enzyme reactions were executed in 0.1 M acetate buffer (pH 4.8) at 50 °C for 10 min, after which the DNS method was used to measure the released reducing sugars. The cellobiohydrolase activity was determined in an acetate buffer (0.1 M) at 50 °C for 30 min with pNPC (Sigma, USA) [62]. One enzyme activity unit was defined as the amount of enzymes required to liberate 1 μmol glucose or pNP per minute under the assayed conditions.

Gene construction of different functional indicators in NJAU4742

Gene deletion and overexpression mutants were obtained via gene replacement strategy using the polyethylene glycol (PEG)-mediated protoplast transformation procedure as described in Zhang et al. [63] with a hygromycin resistance cassette (*HygB*) in wt, or a *ura3* compensation on *ura3*-deleted strain ($\Delta ura3$). The FRET glucose sensors (pDRf1-GW) for monitoring glucose levels in the cytosol were constructed in NJAU4742 according to Hou et al. [64]. The detailed protocols were described in our previous research [47], and all the transformants were screened by PCR with a Phire[®] Plant Direct PCR Kit (Thermo Scientific, USA) and subjected to three rounds of single-spore purification.

Observation of spore germination and vegetative growth

For spore germination, fresh conidia of different strains were adjusted to a concentration of 1×10^6 spores per mL and inoculated on PDA plates for 24 h. As per past practices, spore germination was observed from the 16 h and continued until the 24 h. For vegetative growth, two sterile coverslips were inserted 2 cm away from the inoculated spores on rice straw plates for 48 h, and the coverslips were removed and used for observation after the incubation. All observations and recordings were carried out using a Leica DM2000 (Leica Microsystems Trading Co. Ltd., Germany).

Confocal imaging and fluorescence intensity analysis of glucose sensor

Three-day-old NJAU4742 mycelia were collected using glucose as the sole carbon source. For confocal imaging of glucose, fresh hyphae of different strains with glucose sensor were recorded on a confocal fluorescence microscope (TCS SP8, Leica, Germany) by using a 60× water immersion objective, and the channel of CFP was excited at 456 nm and emitted at 480 nm, while YFP was excited at 488 nm and emitted at 500 nm. The ratios of YFP/CFP were used to evaluate the intracellular glucose content. Data were completed as at least three independent biological replicates. Statistical data were expressed as means ± standard errors (SE) from all valid pixels.

Biolog phenotype microarrays

Growth condition was monitored by using Biolog FF Microplates, which contained 95 different carbon sources in each well and one well with water (BIOLOG, Hayward, USA), as described by Druzhinina et al. [65] with some modifications. Spores were harvested from the 7-day-old PDA cultures and then suspended in milli-Q water, and the concentration was adjusted to 10^7 spores mL⁻¹ using a Biolog turbidity meter at O.D. 590 nm. 90 μL of the spore suspension was dispensed into each well, and the plates were incubated in darkness at 25 °C. The assays were carried out at least with three replicates per genotype, and the values of O.D. 750 nm were measured 12 h to 168 h post-inoculations.

Vacuole morphology observation

The method for identifying vacuole morphology was referred to Chen et al. [66] with some modifications. Briefly, vegetative hyphae of indicated strains were cultured in PDA medium for 48 h. The hyphae were collected and suspended in phosphate buffer (pH 7.0), followed by centrifugation at 4 °C and 1000 rpm for 5 min. The supernatant was discarded, and the pellet was resuspended in phosphate buffer for 15 min, then

centrifuged at 4 °C and 1000 rpm for 5 min. The mycelia were then fixed by adding an appropriate volume of 2.5% glutaraldehyde and 1% paraformaldehyde solution to fully immerse the samples, and they were left at 4 °C overnight for fixation. Afterward, the fungal samples were washed with deionized water and cut into approximately 1 mm thick sections. These sections were dehydrated with a gradient of alcohol, dried, and then coated with a thin layer of gold using a JFC-120 sputter coater. Observation of vacuole morphology was performed with a Hitachi Model H-7650 TEM (Hitachi, Japan).

RNA sequencing and transcriptome analysis

Mycelial samples of strain NJAU4742 intended for RNA sequencing were promptly subjected to RNA extraction using the RNeasy® Plant Mini Kit (Qiagen, Germany). Subsequently, 1% agarose gel electrophoresis was employed to assess the contamination and degradation of the RNA. The qualified RNA samples were subjected to sequencing using the Illumina Novaseq™ 6000 platform (LC-Bio Technology CO., Ltd., Hangzhou, China), and the high quality clean reads were filtered by Cutadapt (version 1.9). Next, the sequencing data were analyzed and compared using the HISAT2 based on the genome of NJAU4742 (<https://bioinfo.njau.edu.cn/tgn4742/>). StringTie (version 1.3.4d) was employed to assemble the mapped reads and estimate the expression levels of transcripts for each sample. Finally, the differential expression of various functional genes was analyzed using edgeR, and the differential expression results were visualized using R language (v4.2.0).

Evaluation of cellular redox state

The ROS assay kit (Beyotime, S0033S) was used to detect the change in ROS levels between different strains inoculated on the rice straw medium plate for 4 days. DCFH-DA was diluted in PBS buffer (pH 7.0) to a final concentration of 10 μmol L⁻¹. The collected mycelia were treated with DCFH-DA for 20 min at 37 °C. After the treatment, the mycelia were washed three times with PBS buffer (pH 7.0) to remove the surface DCFH-DA before measurement. The treated hyphae were observed using a 60× water-immersion objective lens on a confocal fluorescence microscope (TCS SP8, Leica, Germany). The excitation wavelength was set at 488 nm, and the emission wavelength was set at 525 nm. Glutathione redox status is influenced by the total glutathione level and the GSH: GSSG ratio [67]. The glutathione (including GSH and GSSG) of NJAU4742 were quantified by reduced glutathione (GSH) content assay kit (Solarbio, BC1170) and oxidized glutathione (GSSG) content assay kit (Solarbio, BC1180) according to the manufacturer's instructions, respectively. At least three biological replicates were

carried out for each experiment, and the bars indicated the standard error of the replicates.

Apoptosis assay

DAPI staining and caspase-3 assay were performed to verify apoptosis [27]. When stained with DAPI, fungal mycelia were incubated with a DAPI solution (7 μg mL⁻¹) (abcam ab285390) at room temperature for 5 min. A confocal fluorescence microscope (TCS SP8, Leica, Germany) was used for observing and recording with the excitation and emission at 364 nm and 454 nm, respectively. The caspase-3 assay kit (Solarbio, BC3830) was used according to the manufacturer's instructions. Specifically, the respective strains were incubated onto agar plates containing 1.5% straw powder at 28 °C for 3 days. After cultivation, fungal mycelia were collected and thoroughly ground to prepare an extraction solution. The fungal mycelial extract solution was thoroughly mixed with a buffer solution and substrate (DEVD-pNA), followed by incubation at 37 °C for 4 h. The absorbance at 405 nm was measured by a SpectraMax® i3x microplate reader (Molecular Devices, Sunnyvale, CA, USA).

ImageJ analysis

Fluorescence was measured in ImageJ software. Briefly, image colors were extracted through Image-Color-Split Channels, and the RGB format was divided into 8 bit. Auto-threshold was applied to adjust the threshold to avoid exceeding limits, and the intensity analysis was performed by plot profile as previously described by Zhao et al. [68].

Supplementary Information

The online version contains supplementary material available at <https://doi.org/10.1186/s13068-024-02570-w>.

Supplementary Material 1.

Acknowledgements

Not applicable.

Author contributions

T.L. and D.L. designed the experiments. T.L. and Q.W. performed most of the experiments. Y.L., J.W., H.Z., and L.C. assisted in the execution of a subset of experiments. T.L. wrote the manuscript. D.L. and Q.S. assisted in the revision of the manuscript. All authors have read the manuscript and approved the submission to this journal.

Funding

This research was financially supported by National Natural Science Foundation of China (32172680 and 32302679), Natural Science Foundation of Jiangsu Province (BK20230991), the Fundamental Research Funds for the Central Universities (XUEKEN2023039), and the Postdoctoral Fellowship Program of CPSF under Grant (GZC20231126).

Availability of data and materials

No data sets were generated or analysed during the current study.

Declarations**Ethics approval and consent to participate**

Not applicable.

Consent for publication

Agreed by all authors.

Competing interests

The authors declare no competing interests.

Received: 29 November 2023 Accepted: 15 September 2024

Published online: 18 September 2024

References

- Harman GE, Howell CR, Viterbo A, Chet I, Lorito M. *Trichoderma* species—opportunistic, avirulent plant symbionts. *Nat Rev Microbiol*. 2004;2:43–56.
- Vinale F, Sivasithamparan K, Ghisalberti EL, Marra R, Woo SL, Lorito M. *Trichoderma*–plant–pathogen interactions. *Soil Biol Biochem*. 2008;40:1–10.
- Druzhinina IS, Seidl-Seiboth V, Herrera-Estrella A, Horwitz BA, Kenerley CM, Monte E, Mukherjee PK, Zeilinger S, Grigoriev IV, Kubicek CP. *Trichoderma*: the genomics of opportunistic success. *Nat Rev Microbiol*. 2011;9:749–59.
- Gusakov AV. Alternatives to *Trichoderma reesei* in biofuel production. *Trends Biotechnol*. 2011;29:419–25.
- Chukwuma OB, Rafatullah M, Tajarudin HA, Ismail N. Lignocellulolytic enzymes in biotechnological and industrial processes: a review. *Sustainability*. 2020;12:7282.
- Berlin A. No barriers to cellulose breakdown. *Science*. 2013;342:1454–6.
- Lombard V, Golaconda Ramulu H, Drula E, Coutinho PM, Henrissat B. The carbohydrate-active enzymes database (CAZy) in 2013. *Nucleic Acids Res*. 2014;42:D490–5.
- Chandel AK, Chandrasekar G, Silva MB, Silvério da Silva S. The realm of cellulases in biorefinery development. *Crit Rev Biotechnol*. 2012;32:187–202.
- Wang Y, Leng L, Islam MK, Liu F, Lin CSK, Leu S-Y. Substrate-related factors affecting cellulose-induced hydrolysis for lignocellulose valorization. *Int J Mol Sci*. 2019;20:3354.
- Van der Zwan T, Sigg A, Hu J, Chandra RP, Saddler JN. Enzyme-mediated lignocellulose liquefaction is highly substrate-specific and influenced by the substrate concentration or rheological regime. *Front Bioeng Biotechnol*. 2020;8:917.
- Huberman LB, Liu J, Qin L, Glass NL. Regulation of the lignocellulolytic response in filamentous fungi. *Fungal Biol Rev*. 2016;30:101–11.
- Schaller M, Borelli C, Korting HC, Hube B. Hydrolytic enzymes as virulence factors of *Candida albicans*. *Mycoses*. 2005;48:365–77.
- Labbaoui H, Bogliolo S, Ghugtyal V, Solis NV, Filler SG, Arkowitz RA, Bassilana M. Role of Arf GTPases in fungal morphogenesis and virulence. *PLoS Pathog*. 2017;13: e1006205.
- Militello R, Colombo MI. Small GTPases as regulators of cell division. *Commun Integr Biol*. 2013;6: e25460.
- Takai Y, Sasaki T, Matozaki T. Small GTP-binding proteins. *Physiol Rev*. 2001;81:153–208.
- Kahn RA, Cherfils J, Elias M, Lovering RC, Munro S, Schurmann A. Nomenclature for the human Arf family of GTP-binding proteins: ARF, ARL, and SAR proteins. *J Cell Biol*. 2006;172:645–50.
- Kahn RA, Gilman AG. Purification of a protein cofactor required for ADP-ribosylation of the stimulatory regulatory component of adenylate cyclase by cholera toxin. *J Biol Chem*. 1984;259:6228–34.
- Agrawal G, Subramani S. Emerging role of the endoplasmic reticulum in peroxisome biogenesis. *Front Physiol*. 2013;4:286.
- Ackema KB, Hench J, Böckler S, Wang SC, Sauder U, Mergenthaler H, Westermann B, Bard F, Frank S, Spang A. The small GTPase Arf1 modulates mitochondrial morphology and function. *EMBO J*. 2014;33:2659–75.
- Tao C, Wang Z, Liu S, Lv N, Deng X, Xiong W, Shen Z, Zhang N, Geisen S, Li R. Additive fungal interactions drive biocontrol of *Fusarium* wilt disease. *New Phytol*. 2023;238:1198–214.
- Xia Y, Wang J, Guo C, Xu H, Wang W, Yang M, Shen Q, Zhang R, Miao Y. Exploring the multi-level regulation of lignocellulases in the filamentous fungus *Trichoderma guizhouense* NJAU4742 from an omics perspective. *Microb Cell Fact*. 2022;21:1–14.
- Bahn Y-S, Xue C, Idnurm A, Rutherford JC, Heitman J, Cardenas ME. Sensing the environment: lessons from fungi. *Nat Rev Microbiol*. 2007;5:57–69.
- Grimm L, Kelly S, Krull R, Hempel D. Morphology and productivity of filamentous fungi. *Appl Microbiol Biotechnol*. 2005;69:375–84.
- Mukherjee S, Khawala S. Secretion of cellobiase is mediated via vacuoles in *Termitomyces clypeatus*. *Biotechnol Prog*. 2002;18:1195–200.
- Richards A, Veses V, Gow NA. Vacuole dynamics in fungi. *Fungal Biol Rev*. 2010;24:93–105.
- Veses V, Richards A, Gow NA. Vacuoles and fungal biology. *Curr Opin Microbiol*. 2008;11:503–10.
- Zhu H, Li T, Li C, Liu Y, Miao Y, Liu D, Shen Q. Intracellular kynurenine promotes acetaldehyde accumulation, further inducing the apoptosis in soil beneficial fungi *Trichoderma guizhouense* NJAU4742 under acid stress. *Environ Microbiol*. 2023;25:331–51.
- Haddad JJ. A redox microenvironment is essential for MAPK-dependent secretion of pro-inflammatory cytokines: modulation by glutathione (GSH/GSSG) biosynthesis and equilibrium in the alveolar epithelium. *Cell Immunol*. 2011;270:53–61.
- Moley K, Mueckler M. Glucose transport and apoptosis. *Apoptosis*. 2000;5:99–105.
- Mason EF, Rathmell JC. Cell metabolism: an essential link between cell growth and apoptosis. *Biochim Biophys Acta (BBA) Mol Cell Res*. 2011;1813:645–54.
- de Paula RG, Antoniêto ACC, Nogueira KMV, Ribeiro LFC, Rocha MC, Malavazi I, Almeida F, Silva RN. Extracellular vesicles carry cellulases in the industrial fungus *Trichoderma reesei*. *Biotechnol Biofuels*. 2019;12:1–14.
- Tarkka M, Schrey S, Hamp R. Plant associated soil microorganisms. In: *Molecular mechanisms of plant and microbe coexistence*. Berlin: Springer; 2008. p. 3–51.
- Mendoza-Mendoza A, Zaid R, Lawry R, Hermosa R, Monte E, Horwitz BA, Mukherjee PK. Molecular dialogues between *Trichoderma* and roots: role of the fungal secretome. *Fungal Biol Rev*. 2018;32:62–85.
- Liu G, Qu Y. Engineering of filamentous fungi for efficient conversion of lignocellulose: tools, recent advances and prospects. *Biotechnol Adv*. 2019;37:519–29.
- van Peij NN, Gielkens MM, de Vries RP, Visser J, de Graaff LH. The transcriptional activator XlnR regulates both xylanolytic and endoglucanase gene expression in *Aspergillus niger*. *Appl Environ Microbiol*. 1998;64:3615–9.
- Rauscher R, Würleitner E, Waczenovsky C, Aro N, Stricker AR, Zeilinger S, Kubicek CP, Penttilä M, Mach RL. Transcriptional regulation of xyn1, encoding xylanase I, in *Hypocrea jecorina*. *Eukaryot Cell*. 2006;5:447–56.
- Coradetti ST, Craig JP, Xiong Y, Shock T, Tian C, Glass NL. Conserved and essential transcription factors for cellulase gene expression in ascomycete fungi. *Proc Natl Acad Sci*. 2012;109:7397–402.
- de la Serna I, Ng D, Tyler BM. Carbon regulation of ribosomal genes in *Neurospora crassa* occurs by a mechanism which does not require Cre-1, the homologue of the *Aspergillus* carbon catabolite repressor, CreA. *Fungal Genet Biol*. 1999;26:253–69.
- Xiong Y, Sun J, Glass NL. VIB1, a link between glucose signaling and carbon catabolite repression, is essential for plant cell wall degradation by *Neurospora crassa*. *PLoS Genet*. 2014;10: e1004500.
- Montenegro-Montero A, Goity A, Larrondo LF. The bZIP transcription factor HAC-1 is involved in the unfolded protein response and is necessary for growth on cellulose in *Neurospora crassa*. *PLoS ONE*. 2015;10: e0131415.
- Arkowitz RA, Bassilana M. Regulation of hyphal morphogenesis by Ras and Rho small GTPases. *Fungal Biol Rev*. 2015;29:7–19.
- Ma Y, Yang X, Xie M, Zhang G, Yang L, Bai N, Zhao Y, Li D, Zhang K-Q, Yang J. The Arf-GAP AoGlo3 regulates conidiation, endocytosis, and pathogenicity in the nematode-trapping fungus *Arthrobotrys oligospora*. *Fungal Genet Biol*. 2020;138: 103352.

43. Lew RR. How does a hypha grow? The biophysics of pressurized growth in fungi. *Nat Rev Microbiol*. 2011;9:509–18.
44. Riquelme M. Tip growth in filamentous fungi: a road trip to the apex. *Annu Rev Microbiol*. 2013;67:587–609.
45. Kurzątkowski W, Solecka J, Filipek J, Rozbicka B, Messner R, Kubicek C. Ultrastructural localization of cellular compartments involved in secretion of the low molecular weight, alkaline xylanase by *Trichoderma reesei*. *Arch Microbiol*. 1993;159:417–22.
46. Glenn M, Ghosh A, Ghosh BK. Subcellular fractionation of a hypercellulolytic mutant, *Trichoderma reesei* Rut-C30: localization of endoglucanase in microsomal fraction. *Appl Environ Microbiol*. 1985;50:1137–43.
47. Liu Y, Li T, Zhu H, Zhou Y, Shen Q, Liu D. Cysteine facilitates the lignocellulolytic response of *Trichoderma guizhouense* NJAU4742 by indirectly up-regulating membrane sugar transporters. *Biotechnol Biofuels Bioprod*. 2023;16:1–22.
48. Adnan M, Zheng W, Islam W, Arif M, Abubakar YS, Wang Z, Lu G. Carbon catabolite repression in filamentous fungi. *Int J Mol Sci*. 2017;19:48.
49. Biella S, Smith ML, Aist JR, Cortesi P, Milgroom MG. Programmed cell death correlates with virus transmission in a filamentous fungus. *Proc R Soc Lond B*. 2002;269:2269–76.
50. Yorimitsu T, Sato K, Takeuchi M. Molecular mechanisms of Sar/Arf GTPases in vesicular trafficking in yeast and plants. *Front Plant Sci*. 2014;5:411.
51. Williams M, Kim K. From membranes to organelles: emerging roles for dynamin-like proteins in diverse cellular processes. *Eur J Cell Biol*. 2014;93:267–77.
52. Li D, Zhao Z, Huang Y, Lu Z, Yao M, Hao Y, Zhai C, Wang Y. PsVPS1, a dynamin-related protein, is involved in cyst germination and soybean infection of *Phytophthora sojae*. *PLoS ONE*. 2013;8: e58623.
53. Chong X, Wang C, Wang Y, Wang Y, Zhang L, Liang Y, Chen L, Zou S, Dong H. The dynamin-like GTPase FgSey1 plays a critical role in fungal development and virulence in *Fusarium graminearum*. *Appl Environ Microbiol*. 2020;86:e02720-02719.
54. Low HH, Löwe J. A bacterial dynamin-like protein. *Nature*. 2006;444:766–9.
55. Yan S, Xu Y, Tao X-M, Yu X-W. Alleviating vacuolar transport improves cellulase production in *Trichoderma reesei*. *Appl Microbiol Biotechnol*. 2023;107:2483–99.
56. Idiris A, Tohda H, Sasaki M, Okada K, Kumagai H, Giga-Hama Y, Takegawa K. Enhanced protein secretion from multiprotease-deficient fission yeast by modification of its vacuolar protein sorting pathway. *Appl Microbiol Biotechnol*. 2010;85:667–77.
57. Marsalek L, Gruber C, Altmann F, Aleschko M, Mattanovich D, Gasser B, Puxbaum V. Disruption of genes involved in CORVET complex leads to enhanced secretion of heterologous carboxylesterase only in protease deficient *Pichia pastoris*. *Biotechnol J*. 2017;12:1600584.
58. Miao J, Wang M, Ma L, Li T, Huang Q, Liu D, Shen Q. Effects of amino acids on the lignocellulose degradation by *Aspergillus fumigatus* Z5: insights into performance, transcriptional, and proteomic profiles. *Biotechnol Biofuels*. 2019;12:1–19.
59. Xue D, Lin D, Gong C, Peng C, Yao S. Expression of a bifunctional cellulase with exoglucanase and endoglucanase activities to enhance the hydrolysis ability of cellulase from a marine *Aspergillus niger*. *Process Biochem*. 2017;52:115–22.
60. Xiao Z, Storms R, Tsang A. Microplate-based filter paper assay to measure total cellulase activity. *Biotechnol Bioeng*. 2004;88:832–7.
61. Bailey MJ, Biely P, Poutanen K. Interlaboratory testing of methods for assay of xylanase activity. *J Biotechnol*. 1992;23:257–70.
62. Valášková V, Baldrian P. Degradation of cellulose and hemicelluloses by the brown rot fungus *Piptoporus betulinus*—production of extracellular enzymes and characterization of the major cellulases. *Microbiology*. 2006;152:3613–22.
63. Zhang J, Miao Y, Rahimi MJ, Zhu H, Steindorff A, Schiessler S, Cai F, Pang G, Chenthamara K, Xu Y. Guttation capsules containing hydrogen peroxide: an evolutionarily conserved NADPH oxidase gains a role in wars between related fungi. *Environ Microbiol*. 2019;21:2644–58.
64. Hou B-H, Takanaga H, Grossmann G, Chen L-Q, Qu X-Q, Jones AM, Lalonde S, Schweissgut O, Wiechert W, Frommer WB. Optical sensors for monitoring dynamic changes of intracellular metabolite levels in mammalian cells. *Nat Protoc*. 2011;6:1818–33.
65. Druzhinina IS, Schmoll M, Seiboth B, Kubicek CP. Global carbon utilization profiles of wild-type, mutant, and transformant strains of *Hypocrea jecorina*. *Appl Environ Microbiol*. 2006;72:2126–33.
66. Chen Y, Liu J, Fan Y, Xiang M, Kang S, Wei D, Liu X. SNARE protein DdVam7 of the nematode-trapping fungus *Drechslerella dactyloides* regulates vegetative growth, conidiation, and the predatory process via vacuole assembly. *Microbiol Spectr*. 2022;10:e01872-01822.
67. Yu X, Pasternak T, Eiblmeier M, Ditengou M, Kochersperger P, Sun J, Wang H, Rennenberg H, Teale W, Paponov I. Plastid-localized glutathione reductase2-regulated glutathione redox status is essential for *Arabidopsis* root apical meristem maintenance. *Plant Cell*. 2013;25:4451–68.
68. Zhao X, Fang Y, Yang Y, Qin Y, Wu P, Wang T, Lai H, Meng L, Wang D, Zheng Z. Elaiophyllin, a novel autophagy inhibitor, exerts antitumor activity as a single agent in ovarian cancer cells. *Autophagy*. 2015;11:1849–63.

Publisher's Note

Springer Nature remains neutral with regard to jurisdictional claims in published maps and institutional affiliations.